SUST J Sci Tech, Vol 32(2) 2022, 30 - 37 ISSN 1682-895X

CFD Analysis of Blood Flow through Bifurcated Carotid Artery (of Human): Newtonian vs. Non Newtonian Blood Model

(Submitted: 10.09.2022 ; Accepted: 00000000)

Md. Syamul Bashar[1], Rifat Hossain[2], Md. Shafiqul Islam[3]

Shahjalal University of Science and Technology (SUST),
Sylhet, Bangladesh
md.syamul-mee@sust.edu, rifat12@student.sust.edu, msislam-mee@sust.edu

Abstract

Blood behaves like either a Newtonian or Non-Newtonian fluid depending on the shear stress it experiences. In the current study, a 3D model of a human bifurcated carotid artery was used to get insights into the differences between Newtonian and Non-Newtonian blood flow. As the experimental or numerical setup will be made simpler by representing blood as a Newtonian fluid. We are interested in whether it makes sense to represent blood as a Newtonian fluid. Fluent (ANSYS, 15) software was used to run two different simulations, one for blood as a Newtonian fluid and the other for a Non-Newtonian fluid. The Carreau model has been used to define the Non-Newtonian behavior of blood. A qualitative and quantitative comparison of Newtonian and Non-Newtonian blood flow has been done based on blood velocity, pressure, and wall shear stress (WSS). All comparisons were done at the minimum and maximum intake velocities of a cardiac cycle. To evaluate how close Newtonian and Non-Newtonian results are a root mean square error (RMSE) calculation has been done. At the time of minimum inlet velocity, the differences between the corresponding Newtonian and Non-Newtonian values ranged from zero to small. Additionally, the differences between corresponding Newtonian and Non-Newtonian velocities lessen at maximum inlet velocity. The impacts of blood's Non-Newtonian behavior have been found minimal. Blood may be modeled as a Newtonian fluid for simplicity in the experimental or numerical analysis of blood flow through the carotid artery, with minimal error.

Keywords: Computational Fluid Dynamics; Bifurcated Carotid Artery; Newtonian Fluid; Non-Newtonian Fluid; Wall Shear Stress.

1. Introduction

Arteries are blood vessels that carry oxygenated blood to the tissues of our body. Carotid arteries are blood vessels in the neck, supply oxygenated blood to the brain, neck, face, etc. At some point in the neck, the carotid artery splits into the internal carotid artery (ICA) and external carotid artery (ECA). A widening of a carotid artery at its main branch point is known as sinus. After which ICA is located. The function of the ICA is to supply oxygenated blood to the brain, including the eyes [1]. And ECA supplies blood to the face, neck, etc. Proper functioning of the carotid arteries is essential. Some of the conditions of carotid arteries are carotid artery aneurysm, carotid artery stenosis, carotid artery atherosclerosis, etc. Due to higher blood pressure and, or weak artery wall, a small area of blood vessels may bulge outward, which is an aneurysm condition. Regions which experience low or oscillatory shear stress are susceptible to fat, cholesterol, etc. accumulation known as atherosclerosis [2]. The development and progression of atherosclerotic plaques are significantly influenced by hemodynamic patterns such as low WSS, secondary flows, and recirculation zones [3] [4] [5]. To simulate above mentioned conditions related to the carotid artery, it is essential to choose the right viscosity model. And, there is no definitive answer to this question. Human blood exhibits shear thinning behavior, which is sort of a Non-Newtonian property [6]. Additionally, at $\tau > 1.5$ dynes/cm^2, blood displays Newtonian behavior [7]. Different models may be more appropriate for different situations. Some common Non-Newtonian viscosity models for blood include the Herschel-Bulkley model, the Casson model, the Modified Power Law-Cross model (MPL-Cross), and the Carreau model. Numerous studies have been conducted to discover the better suitable viscosity model for blood. Using the Newtonian model for the blood flow didn't produce promising results in blocked areas and beyond them, according to [8], they simulated blood flow through a moderately stenotic femoral artery bifurcation. According to [9], a Non-Newtonian model is more appropriate to examine transient blood flow in greater detail through the right coronary artery and the usage of the Newtonian blood model is a reasonable approximation. And from the

Copyright © 201x SUST

study of [10], there were no disparities between the flow behaviors predicted by the Casson model and the flow characterizations obtained by the Newtonian model. And the discrepancies mostly show up in the area of low shear rates and flow recirculation zones. The Casson model performs better than the Herschel-Bulkley model at simulating the Non-Newtonian properties of blood viscosity according to the study of [11]. And, The MPL-Cross model is less susceptible to changes in flow rate than the Carreau model [12]. The above discussion about different Non-Newtonian viscosity models concludes it is a reasonable choice to use the Carreau model for modeling the Non-Newtonian behavior of blood.

In the current work, a 3D bifurcated carotid artery was designed using SolidWorks 2017 software before the simulation environment was set up. The model geometry's basic dimensions were acquired from Bharadvaj et al., 1982. (See section 2.1 for details). Ansys Fluent 2015, which uses the finite volume method (FVM) to solve fluid fields numerically, was used to prepare the simulation environment (See section 2.4 for details). A validation test has been carried out in advance of the simulations of interest to support our simulation methodology (See section 2.2 for details). Utilizing Ansys CFD Post, the results (Velocity, Pressure, and Wall Shear Stress distribution) were all extracted. Python programming language has been used to plot the velocity, pressure, and WSS distribution graph. To find out the differences between Newtonian and Non-Newtonian behavior of blood, we have done a qualitative analysis (See sections 3.1.1, 3.1.2, and 3.1.3). Finally, a quantitative analysis has been done to numerically assess the differences between corresponding Newtonian and Non-Newtonian results more precisely. For the qualitative study, we have chosen the bifurcation plane and its perpendicular planes at SS3 and EC2. As the SS3 and EC2 perpendicular cross-sections are the largest in the ICA and ECA, respectively. And these areas are anticipated to experience reduced velocity and somewhat increased pressure that is associated with atherosclerosis. As from visual inspections of velocity contours (See fig. 4, fig. 5, fig. 6) no significant differences have been observed between corresponding Newtonian and Non-Newtonian velocity distribution. To find out the differences between corresponding Newtonian and Non-Newtonian data more precisely, absolute minimum and maximum differences between related outcomes (see table 1) as well as the RMSE (see table 2) have been calculated to assess how well Newtonian and Non-Newtonian results coincide or differ.

2. Methodology

To solve the blood flow field Continuity equation and Navier-stokes equation has been assigned in Ansys Fluent, 15.

The Continuity equation:

$$\nabla.\mathrm{U}= 0, \frac{\partial u}{\partial x}+\frac{\partial v}{\partial y}+\frac{\partial w}{\partial z}= 0 \quad (1)$$

Where, U represents total velocity, and u, v, w are velocity components in x, y, z directions, respectively.

Navier-stokes equation:

$$\rho\frac{d\overline{V}}{dt}= -\nabla p+ \mu\nabla^2\overline{V}+ \rho g \quad (2)$$

Where, $\overline{V}$, ρ, μ, g represent total velocity, density, viscosity, and gravitational acceleration respectively.

2.1 Geometric Model Construction

The geometric model's dimensions were taken from Bharadvaj et al., 1982. excluding the angle of the bifurcation. It is symmetrical about the common carotid artery (CCA) axis and was taken 40 degrees. The CCA length was set at 130 mm because that is the typical length for CCA, according to Bharadvaj et al., 1982. Using the SolidWorks 2017 program, the geometric model was created.

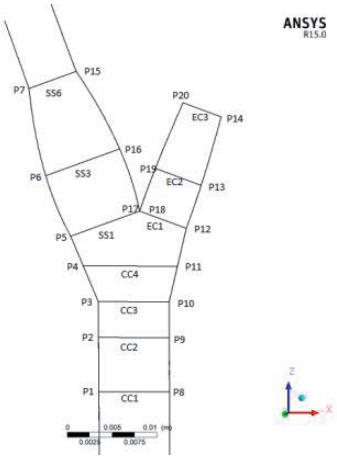

Fig. 1: Bifurcation plane of the 3D model arteries.

2.2 Validation and Grid Independency Test

For the geometric model, a test for grid independence was conducted. For meshing, tetrahedron cells are used. There were 696328 nodes and 389467 elements in the mesh. The experiment from Bharadvaj et al., 1982 has been simulated for validation purposes of our work. As well as compared the simulated outcomes to those from Bharadvaj et al., 1982. Between the results of the experiment and the results of the simulation, there is a good agreement. The velocity profiles at the CC3 line and SS3 line are shown in fig. 2(a), and 2(b), respectively. Additionally, all the cases had a 70:30 outflow ratio with upstream Reynolds numbers of 400, and 800, respectively. Additionally, blood viscosity and blood density have been taken 0.0035 kg/m-s and 1050 kg/m^3, respectively. Artery wall was considered as rigid in the simulation.

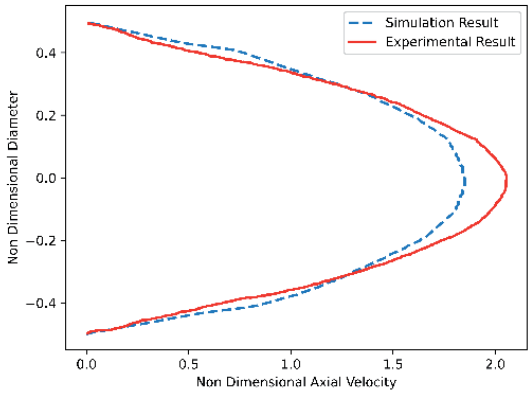

(a) At CC3 line.

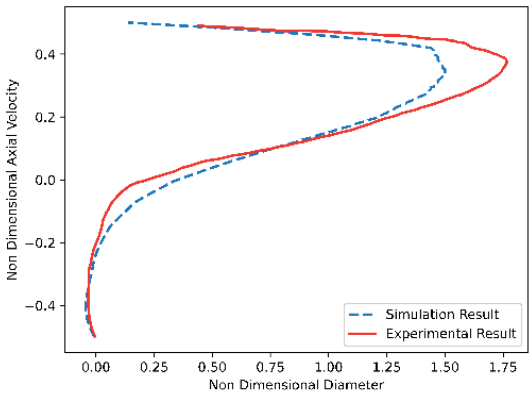

(b) At SS3 line.

Fig. 2: Numerical Validation of Bharadvaj et al., 1982 [13].

2.3 Fluid Property

Blood has been modeled as Newtonian fluid and Non-Newtonian fluid respectively. For the Newtonian case, blood viscosity has been taken 0.0035 kg/m-s. And for the Non-Newtonian case, to define blood viscosity, the Carreau model has been assigned. And blood density for both cases is taken 1050 kg/m^3.

Carreau model: $\frac{\mu-\mu_\infty}{\mu_0-\mu_\infty} = [1 + (\lambda\gamma)^2]^{\frac{n-1}{2}}$ (3)

Where μ_∞= 0.0035 kg/m-s, μ_0= 0.056 kg/m-s, n = 0.3568 and λ= 3.313 s [14]

2.4 Numerical Method

Software called Fluent (ANSYS 15) was used to solve the governing equations mentioned earlier. Fluent solves fluid flow fields numerically using the finite volume approach. As a viscous model, the large eddy simulation has been used, and the transient formulation is based on the bounded second-order implicit option. The simulation was run over six cardiac cycles and the cardiac cycle was divided into 86 equal time segments. The simulation's convergence was based on the residual in continuity falling below 10^{-6} for each time step. The velocity variations between succeeding cycles, under those circumstances, were less than 10^5.

2.5 Boundary Conditions

At the CCA's inlet, the cardiac cycle shown in fig. 3 was specified. The time period of the cardiac cycle is 0.857 seconds. Minimum and maximum velocities on the cardiac cycles are at .27s (t_2) and .33s (t_4) respectively. At the outlet of the ICA and ECA, the outflow was 70% and 30% respectively. No-slip boundary conditions are imposed on the carotid artery bifurcation's walls, which are regarded as rigid walls.

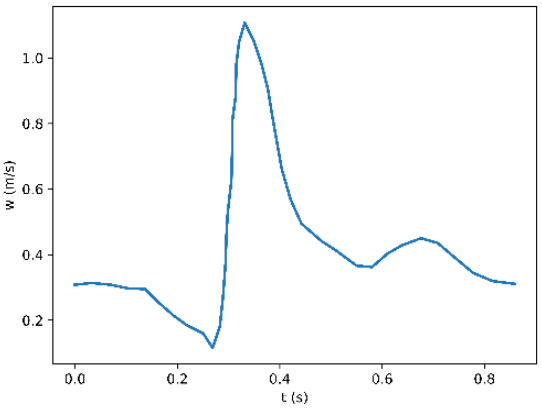

Fig. 3: Flow waveform as a boundary condition at CCA inlet. [15]

3. Results and discussion

3.1.1. Qualitative Velocity Distribution Analysis on the Bifurcation Plane

After the sinus section, there has been an increase in velocity for both the Newtonian and Non-Newtonian cases (at t_4), and a secondary flow zone has formed close to the sinus' outer wall. Additionally, a separate secondary flow zone has been observed near the ECA's outer wall considerably less than the sinus has.

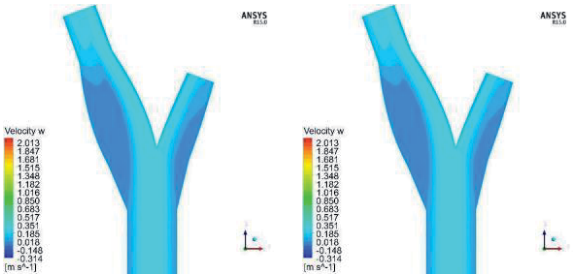

(a) Newtonian Flow at t_2 (b)Non-Newtonian Flow at t_2

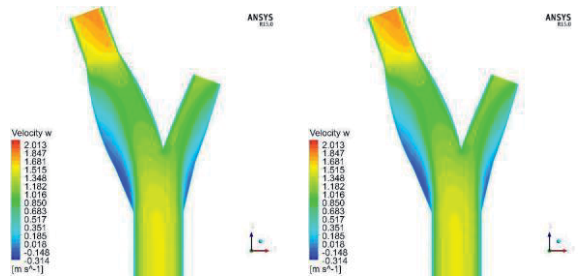

(c) Newtonian Flow at t_4 (d)Non-Newtonian Flow at t_4

Fig. 4: Velocity Distribution Profile on the Bifurcation Plane.

3.1.2. Qualitative Velocity Distribution Analysis on the Perpendicular Plane (at SS3) of the Bifurcation Plane

Due to the secondary flow zone near the outer wall, a shift in the velocity profile towards the sinus internal wall has been seen in both cases.

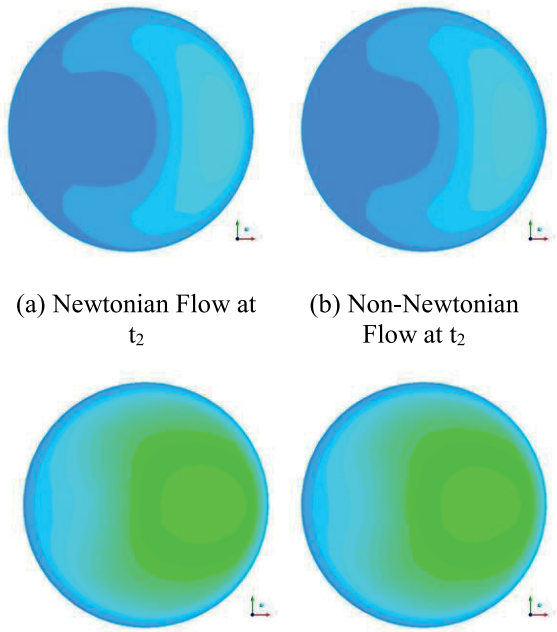

(a) Newtonian Flow at t_2 (b) Non-Newtonian Flow at t_2

(c) Newtonian Flow at t_4 (d) Non-Newtonian Flow at t_4

Fig. 5: Velocity Distribution Profile on Perpendicular Plane (at SS3) of the Bifurcation Plane.

3.1.3. Qualitative Velocity Distribution Analysis on the Perpendicular Plane (at EC2) of the Bifurcation Plane

Due to the presence of a secondary flow zone close to the outer wall, the cross-section at ECA also experienced a shift in the velocity profile in the direction of the internal wall.

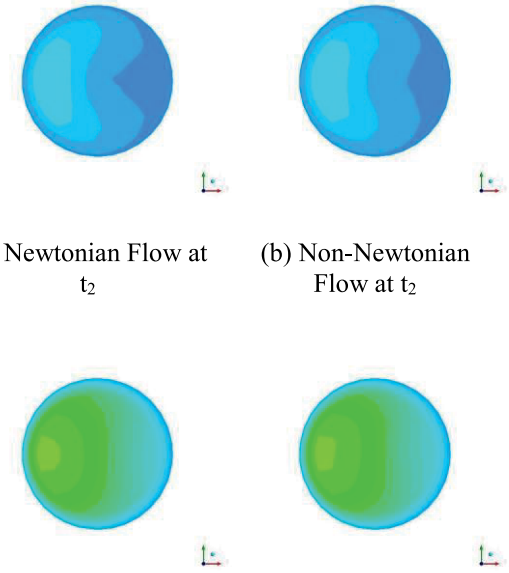

(a) Newtonian Flow at t_2 (b) Non-Newtonian Flow at t_2

(c) Newtonian Flow at t_4 (d) Non-Newtonian Flow at t_4

Fig. 6: Velocity Distribution Profile on Perpendicular Plane (at EC2) of the Bifurcation Plane.

3.2. Quantitative Analysis of Velocity Distribution

The maximum and minimum absolute differences between corresponding Newtonian and Non-Newtonian velocities have been calculated (Table 1), at the points on the EC2 and SS3 lines where maximum or minimum differences have been found. In Table 2, the RMSE values have also been calculated to determine the discrepancy between Newtonian values and Non-Newtonian values. A similar calculation has been performed for pressure as well. And Differences between corresponding WSS were very close to zero.

Table 1: Newtonian Vs. Non -Newtonian Quantitative Comparison: Absolute Differences Calculation

		At EC2 line		At SS3 line	
		t_2	t_4	t_2	t_4
Velocity Diff. (m/s)	Max.	.0278	.025	.0496	.029
	Min.	0	0	0	0
Pressure Diff. (Pa)	Max.	3.0	3.0	2.50	4.0
	Min.	2.6	0	1.6	1

Table 2: Newtonian Vs. Non-Newtonian Quantitative Comparison: RMSE Calculation

		At EC2 line		At SS3 line	
		t_2	t_4	t_2	t_4
RMSE	Velocity	0.01512	0.00873	0.01844	0.01300
	Pressure	2.8294	1.6093	2.0527	3.0798

3.2.1. Velocity Distribution at SS3

A larger backflow region has been estimated by the Newtonian model near the outer wall of the sinus section. Additionally, the maximum velocity has also been calculated for the Newtonian case (See fig. 7 (a)).

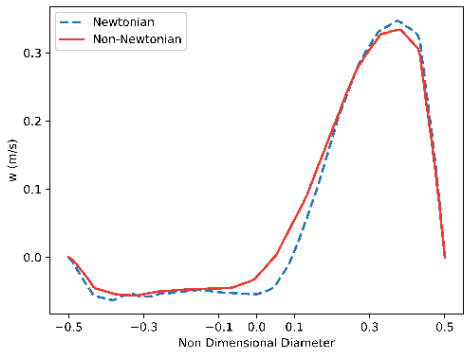

(a) At t_2

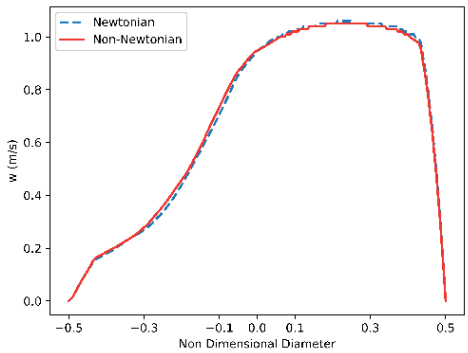

(b) At t_4

Fig. 7: Velocity Distribution Profile on SS3 line of the Bifurcation Plane.

3.2.2. Velocity Distribution at EC2

The Newtonian model has estimated both the maximum and minimum velocities (See fig. 8 (a)). The Newtonian model additionally exhibits a backflow close to the ECA outer wall at t_2. The Non-Newtonian case, however, has not shown any backflow.

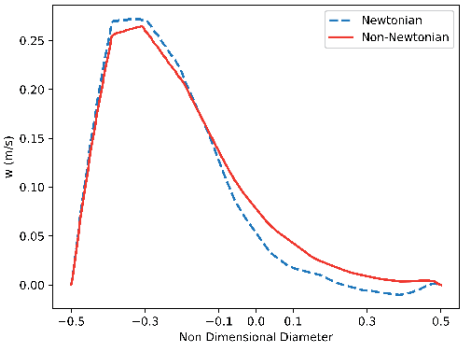

(a) At t_2

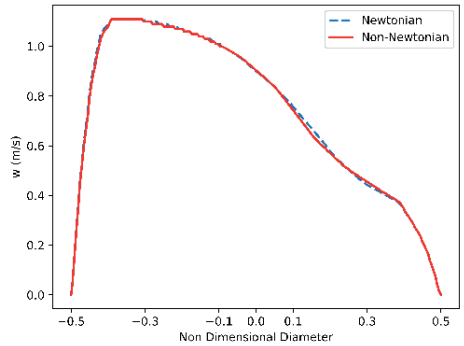

(b) At t_4

Fig. 8: Velocity Distribution Profile on EC2 line of the Bifurcation Plane.

3.3. Quantitative Analysis of Pressure Distribution

3.3.1. Pressure Distribution at SS3

The Newtonian model and the Non-Newtonian model, respectively, have estimated higher pressure at t_2 and t_4.

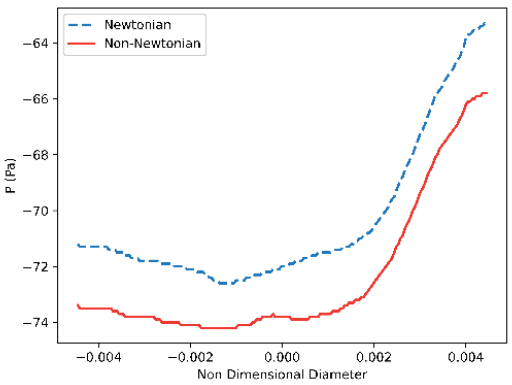

(a) At t_2

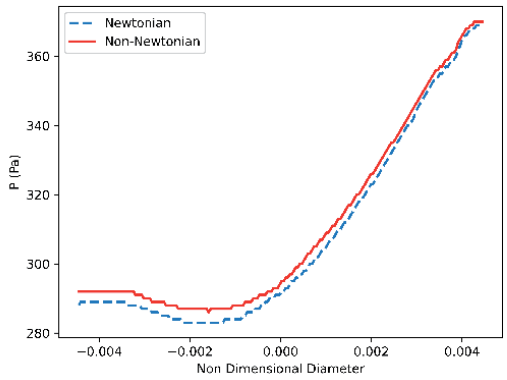

(b) At t_4

Fig. 9: Pressure Distribution Profile on SS3 line of the Bifurcation Plane.

3.3.2. Pressure Distribution at EC2

Higher pressure has been estimated by the Newtonian model and Non-Newtonian model at t_2 and t_4 respectively.

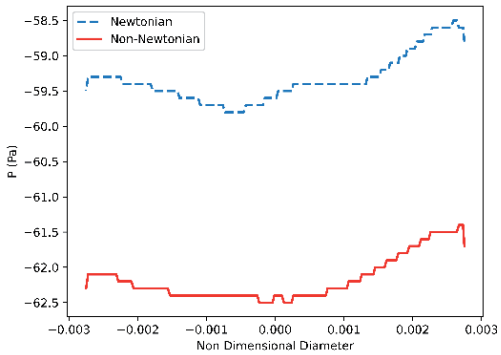

(a) At t_2

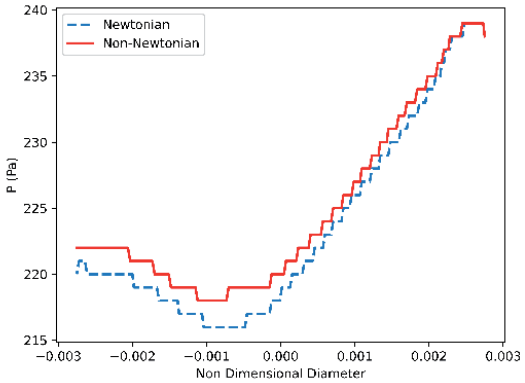

(b) At t_4

Fig. 10: Pressure Distribution Profile on EC2 line of the Bifurcation Plane.

3.4. Wall Shear Stress (WSS) Analysis

3.4.1. Shear Stress Distribution along Left Inner Wall

In this particular case, both Newtonian and Non-Newtonian models have almost the same estimation of WSS.

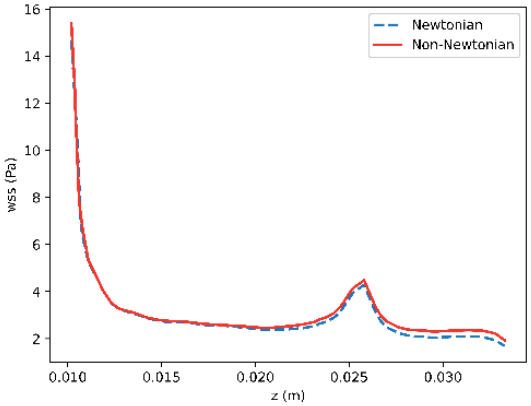

(a) At t_2

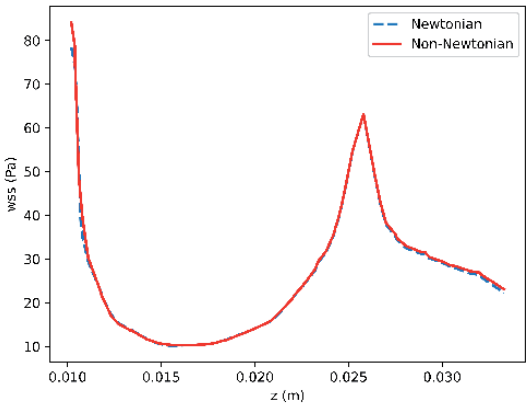

(b) At t_4

Fig. 11: Wall Shear Stress Distribution Profile along L.I.W.

3.4.2. Shear Stress Distribution along Left Outer Wall

A maximum WSS has been estimated by the Non-Newtonian model (at t_2).

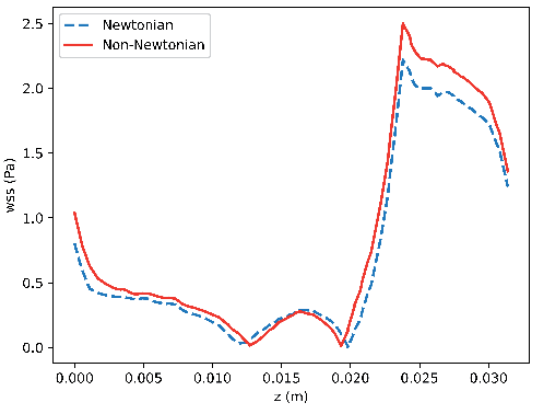

(a) At t_2

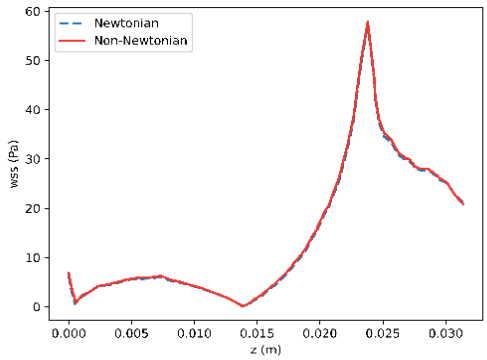

(b) At t_4

Fig. 12: Wall Shear Stress Distribution Profile along L.O.W.

3.4.3. Shear Stress Distribution along Right Inner Wall

Along the right inner wall, both models have shown almost the same WSS value.

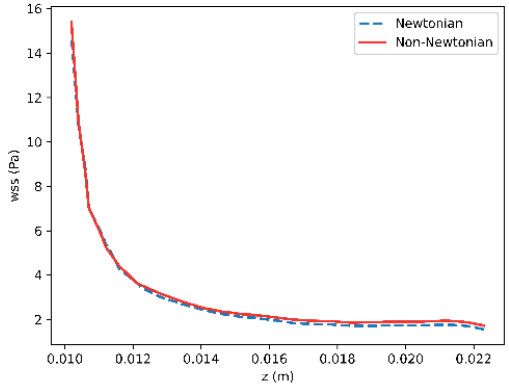

(a) At t_2

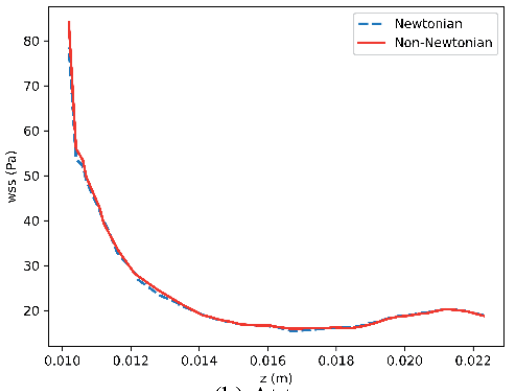

(b) At t_4

Fig. 13: Wall Shear Stress Distribution Profile along R.I.W.

3.4.4. Shear Stress Distribution along Right Outer Wall

The Non-Newtonian model has estimated a little higher WSS along the right outer wall (at t_2).

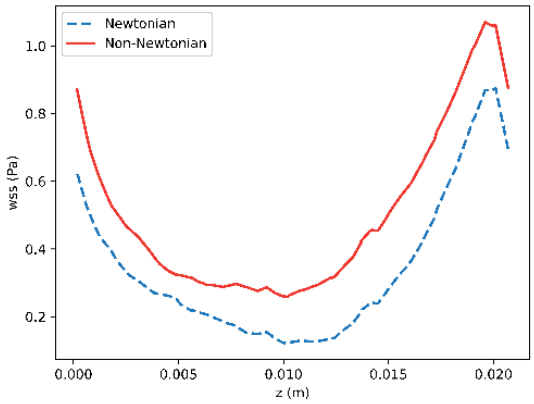

(a) At t_2

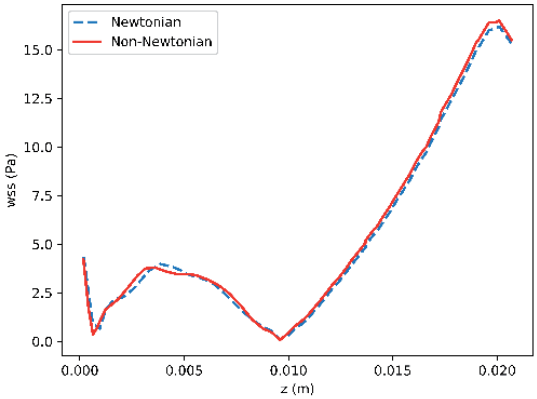

(b) At t_4

Fig. 14: Wall Shear Stress Distribution Profile along R.O.W.

5. Conclusion

The goal of this study is to assess whether it is reasonable to model blood as a Newtonian fluid. As it will be simpler to perform experimental and numerical studies on blood flow if blood is modeled as a Newtonian fluid. Visual inspection of the velocity contours (See sections 3.1.1, 3.1.2, and 3.1.3) revealed no obvious variations between the Newtonian and Non-Newtonian models, so we shifted our attention to quantitative analysis. In quantitative analysis, velocity differences were found to range from 0 to 0.0496 m/s, and pressure differences range from 0 to 4 pa (See table 1). Furthermore, the maximum RMSE values for the corresponding pressure curves were 3.0798 and 0.01844 for the corresponding velocity curves, respectively (See table 2). For corresponding pressure curves RMSE values were a bit higher compared to corresponding velocity curves. A lower RMSE number indicates better agreement between results obtained using Newtonian and non-Newtonian approaches. Based on the visual inspection and RMSE values, utilizing the Newtonian viscosity model, in the case of qualitative study is

reasonable. And, it is advisable to utilize the best Non-Newtonian viscosity model available if the research findings need to be accurate to a high degree. The limitations of this study include that the artery wall was assumed as rigid, the outflow ratio was fixed at 70:30, and a flow waveform would have been a more suitable outflow boundary condition. Additionally, there will be significant individual differences in the size of bifurcated arteries and boundary conditions. Blood hemodynamics may be changed by these factors. This can therefore result in a different conclusion to our study question. By addressing these issues with the current study's design, future research will provide a more confident interpretation.

Acknowledgment

We are highly appreciative of the computational lab facilities provided by the Department of Mechanical Engineering at SUST.

References:

1. Kiel, Jeffrey W. (2011). The Ocular Circulation. Colloquium Series on Integrated Systems Physiology: From Molecule to Function, 3(1), 1–81.

2. Bharadvaj, B.K. Mabon, R.F. & Giddens, D.P. (1982). Steady flow in a model of the human carotid bifurcation. Part I—Flow visualization. J. Biomechanics, 15(5), 349–362.

3. Zhao, S.Z., X.Y. Xu, A.D. Hughes, S.A. Thom, A.V. Stanton, B. Ariff and Q. Long, 2000, Blood flow and vessel mechanics in a physiologically realistic model of a human carotid arterial bifurcation, J. of Biomech. 33, 975-984.

4. Malek. A.M., S.L Alper and S. Izumo, 1999, Hemodynamic shear stress and its role in atherosclerosis, JAMA 282, 2035-2042.

5. Buchmann, N.A. and M.C. Jermy, 2008, Blood flow measurements in idealized and patient specific models of the human carotid artery, 14th Int. Symp. On Applications of Laser Techniques to Fluid Mechanics, Lisbon, Portugal, 1-11.

6. Gijsen, F.J.H., Allanic, E., van de Vosse, F.N. & Janssen, J.D. (1999). The influence of the non-Newtonian properties of blood on the flow in large arteries: unsteady flow in a 90° curved tube. Journal of Biomechanics, 32(7), 705–713.

7. Merrill, E W & Pelletier, G A (1967). Viscosity of human blood: transition from Newtonian to non-Newtonian. Journal of Applied Physiology, 23(2), 178–182.

8. Amiri, Mohammad Hassan; Keshavarzi, Ahmad; Karimipour, Arash; Bahiraei, Mehdi; Goodarzi, Marjan; Esfahani, J. A. (2019). A 3-D numerical simulation of non-Newtonian blood flow through femoral artery bifurcation with a moderate arteriosclerosis: investigating Newtonian/non-Newtonian flow and its effects on elastic vessel walls. Heat and Mass Transfer, (), – . doi:10.1007/s00231-019-02583-4

9. Barbara M. Johnston; Peter R. Johnston; Stuart Corney; David Kilpatrick (2006). Non-Newtonian blood flow in human right coronary arteries: Transient simulations. , 39(6), 1116–1128. doi:10.1016/j.jbiomech.2005.01.034

10. Fan, Y., W. Jiang, Y. Zou, J. Li, J. Chen and X. Deng, 2009, Numerical simulation of pulsatile non Newtonian flow in the carotid artery bifurcation, Acta Mech Sin. 25, 249-255.

11. Lee, B.K., S. Xue, J.H. Nam, H.J. Lim and S.H. Shin, 2011, Determination of blood viscosity and yield stress with a pressure-scanning capillary emorheometer using constitutive models, Korea-Aust. Rheol. J. 23, 1-6.

12. Dosunmu, Idowu T., Shah, Subhash N. (2015). Pressure drop predictions for laminar pipe flow of carreau and modified power law fluids. The Canadian Journal of Chemical Engineering, 93(5), 929–934. doi:10.1002/cjce.22170

13. B.K. Bharadvaj; R.F. Mabon; D.P. Giddens (1982). Steady flow in a model of the human carotid bifurcation. Part II—Laser-Doppler anemometer measurements., 15(5), 363–378. doi:10.1016/0021-9290(82)90058-6

14. Shibeshi, Shewaferaw S.; Collins, William E. (2005). The Rheology of Blood Flow in a Branched Arterial System. Applied Rheology, 15(6), 398–405. doi:10.1515/arh-2005-0020

15. Seo, Taewon (2013). Numerical simulations of blood flow in arterial bifurcation models. Korea-Australia Rheology Journal, 25(3), 153–161. doi:10.1007/s13367-013-0016-7